

circulators are proposed. Some of the problems of actual implementations are discussed.

#### REFERENCES

- [1] S. T. Peng, T. Tamir, and H. L. Bertoni, "Theory of periodic dielectric waveguides," *IEEE Trans. Microwave Theory Tech.*, vol. MTT-23, pp. 123-133, Jan. 1975.
- [2] J. A. Harris, R. K. Winn, and D. G. Dalgoutte, "Theory and design of periodic couplers," *Appl. Opt.*, vol. 11, pp. 2234-2241, Oct. 1972.
- [3] K. Ogawa and W. S. C. Chang, "Analysis of holographic thin film grating coupler," *Appl. Opt.*, vol. 12, pp. 2167-2171, Sept. 1973.
- [4] T. Itoh, "Application of gratings in a dielectric waveguide for leaky-wave antennas and band-reject filters," *IEEE Trans. Microwave Theory Tech.*, vol. MTT-25, pp. 1134-1138, Dec. 1977.
- [5] B. S. Song and T. Itoh, "Distributed Bragg reflection dielectric waveguide oscillators," *IEEE Trans. Microwave Theory Tech.*, vol. MTT-27, pp. 1019-1022, Dec. 1979.
- [6] K. Handa, S. T. Peng, and T. Tamir, "Improved perturbation analysis of dielectric gratings," *Appl. Phys.*, vol. 5, pp. 325-328, Jan. 1975.
- [7] K. Araki, T. Koyama, and Y. Naito, "Reflection problems in a ferrite stripline," *IEEE Trans. Microwave Theory Tech.*, vol. MTT-24, pp. 491-498, Aug. 1976.
- [8] V. P. Nanda, "A new form of ferrite device for millimeter-wave integrated circuits," *IEEE Trans. Microwave Theory Tech.*, vol. MTT-24, pp. 876-879, Nov. 1976.
- [9] M. Tsutsumi, T. Ohira, T. Yamaguchi, and N. Kumagai, "Reflection of millimeter waves by a corrugated dielectric slab waveguide," *Proc. IEEE*, to be published.
- [10] K. Araki, S. Enjohji and Y. Naito, "A simplified analysis of ferrite-strip," *Trans. Inst. Electron. Commun. Eng. Japan*, vol. 63-B, pp. 211-217, Mar. 1980.



Kiyomichi Araki was born in Nagasaki, Japan, on January 7, 1949. He received the B.S. degree in electrical engineering in 1971 from Saitama University, Urawa, Japan and the M.S. and Ph.D. degrees in physical electronics both from Tokyo Institute of Technology, Tokyo, Japan in 1973 and 1978, respectively.

Since April 1978, he has been with Tokyo Institute of Technology. From September 1979 to August 1980, he was a Visiting Research Associate at the University of Texas, Austin, Texas. His research interest is mainly in the microwave and millimeterwave integrated circuits.

Dr. Araki is a member of the Institute of Electronics and Communication Engineers of Japan.

+

**Tatsuo Itoh** (S'69-M'69-SM'74), for a photograph and biography please see page 842 of this issue.

# Fundamental Considerations in Millimeter and Near-Millimeter Component Design Employing Magnetoplasmons

DONALD M. BOLLE, SENIOR MEMBER, IEEE, AND SALVADOR H. TALISA, MEMBER, IEEE

**Abstract**—The feasibility of using surface magnetoplasmons on semiconducting substrates to obtain circuit functions which match those of ferrite loaded devices at lower frequencies, is investigated. This article

describes some initial results obtained in our study of performance characteristics using the best loss parameters available for GaAs materials. Canonical models are considered which relate directly to proposed configurations for differential phase shifters and isolators in the millimeter and near-millimeter ranges.

## I. INTRODUCTION

**A** N INVESTIGATION is presented on the feasibility of using the properties of surface magnetoplasmons on semiconducting substrates as a basis for developing

Manuscript received December 8, 1980; revised April 27, 1981. This work was supported by the Office of Naval Research under Contract N00014-75-C-0750.

The authors are with the Department of Electrical and Computer Engineering, Lehigh University, Packard Laboratory #19, Bethlehem, PA 18015.

planar integrated nonreciprocal devices such as isolators, phase shifters, switches, directional couplers, and circulators, in the millimeter and near-millimeter wave ranges.

A high quality, moderately doped n-type GaAs material has been taken as the substrate, with a carrier concentration ( $n \approx 10^{15} \text{ cm}^{-3}$ ) equivalent to a plasma frequency  $\omega_p = 10^{13} \text{ rad/s}$ . At liquid nitrogen temperatures, mobilities of the order of  $2 \times 10^5 \text{ cm}^2/\text{V}\cdot\text{s}$  can be obtained. This is equivalent to a momentum relaxation time of  $\tau = 8 \times 10^{-12} \text{ s}$ . Losses in the semiconductor will then be modeled by this parameter, since at these low temperatures the effects of lattice vibrations can be neglected.

For the range of frequencies of interest to us, the interaction of the material with the applied electromagnetic field is well described by the local theory of plasmas (Drude model) [1]–[3]. Considering the semiconductor as a dielectric medium which becomes anisotropic upon exposure to a uniform dc magnetic field, the isotropic case will then be a simplification of this general situation.

The semiconducting material is characterized by a permittivity tensor  $\epsilon(\omega)$ . Use of the local theory implies the following assumptions [4]:

- the dielectric tensor at a given point in the medium is independent of the proximity to the surface;
- the wave-vector dependence of the dielectric tensor is neglected;
- any interaction with optical phonons is neglected.

The first two assumptions can be made because the wavelengths of interest will be much larger than the lattice spacing and the carrier mean free path. This third assumption is reasonable for frequencies much less than the transverse optical phonon frequency. The contribution to the dielectric tensor elements from the lattice is then reduced to  $\epsilon^{(0)}$ , the static dielectric constant of the material.

In addition to these assumptions and consistent with Drude's theory, a collision frequency  $\nu = 1/\tau$  is included in the expression of the dielectric tensor, which models the losses in the semiconducting material.

For a biasing magnetic field in the  $y$ -direction, the dielectric tensor takes the following form:

$$\epsilon(\omega) = \begin{bmatrix} \xi & 0 & -j\eta \\ 0 & \xi & 0 \\ j\eta & 0 & \xi \end{bmatrix} \quad (1)$$

where

$$\xi = \epsilon^{(0)} - \frac{\omega_p^2(\omega - j\nu)}{\omega[(\omega - j\nu)^2 - \omega_c^2]} \quad (2)$$

$$\eta = \frac{-\omega_p^2 \omega_c}{\omega[(\omega - j\nu)^2 - \omega_c^2]} \quad (3)$$

$$\zeta = \epsilon^{(0)} - \frac{\omega_p^2}{\omega(\omega - j\nu)} \quad (4)$$

and  $\omega_c$  is the cyclotron frequency  $\omega_c = eB_0/m^*$ .

Note that in the isotropic case  $\omega_c = 0$  and the tensor

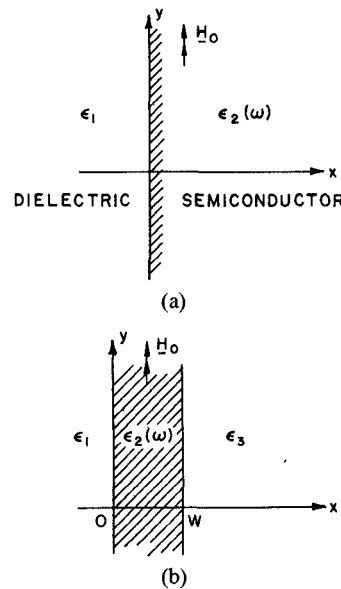


Fig. 1. (a) Single dielectric-semiconductor interface structure. (b) Semiconducting slab sided by dielectric.

elements reduce to

$$\xi = \zeta = \epsilon^{(0)} - \frac{\omega_p^2}{\omega(\omega - j\nu)} \quad (5)$$

$$\eta = 0.$$

Results of theoretical and experimental research on surface plasmons and magnetoplasmons have been extensively reported in the literature, particularly in connection with a single dielectric–plasma interface [4]–[16]. Economou [5] has considered also other simple structures for the isotropic case such as a slab of plasma placed in vacuum or an air gap in a plasma (see also [17] and [18]).

May *et al.* [19]–[23] have reported the design and construction of Faraday rotation isolators and circulators and reflection beam isolators for the millimeter and far-infrared wave ranges using magnetoplasmons in semiconductors.

In the present work, two basic geometries are studied (see Fig. 1)—A dielectric–semiconductor single interface and an infinite semiconducting slab sided by dielectric materials of equal or different permittivities.

Since results concerning the isotropic case have been presented elsewhere [24], we restrict our consideration to the anisotropic case. Furthermore, only the situation in which the biasing magnetic field is parallel to the interface and normal to the direction of propagation is studied. This case has been shown [4], [6]–[11] to give a dispersion ( $\omega - \beta$ ) diagram which is nonreciprocal with respect to the direction of propagation, thus offering possibilities for design of devices. This same idea was previously pursued for ferrite devices [25]–[27].

In most of the work reported in the literature, however, materials are used that have plasma frequencies much higher than those of interest to us. Furthermore, the range of frequencies relative to both the plasma frequency  $\omega_p$  and the cyclotron frequency  $\omega_c$  is often not the same as that of interest here. Therefore, we present our own results for the

case of a single dielectric-plasma interface with  $\omega_p = 10^{13}$  rad/s and  $\omega_c = 10^{12}$  rad/s, equivalent to a magnetic field of 3810 G. These values have been used throughout this study. It should be noted that  $\omega_c \tau > 1$ . This is a condition for an effective interaction between the material and the electromagnetic field.

## II. THE SEMI-INFINITE STRUCTURE

In this analysis the semiconducting material is first assumed to be lossless ( $\nu=0$ ). The effects of collisions will be considered in the next section.

Making use of expressions (1) through (4), we solve Maxwell's equations for the geometry of Fig. 1(a) where we assume that a uniform dc magnetic field  $B_0$  is applied in the  $y$ -direction. With no variations of the fields in this direction, the only solution that allows for transverse confinement in the vicinity of the interface is a TM mode (components  $H_y, E_x, E_z$ ). The transverse behavior of the fields is to be described by  $e^{k_1 x}$  and  $e^{-k_2 x}$  in the dielectric and semiconductor sides, respectively, with

$$\operatorname{Re}[k_1] > 0 \quad \operatorname{Re}[k_2] > 0. \quad (6)$$

The dispersion relation obtained from matching the boundary conditions at the interface is

$$k_2 + j\gamma\eta/\xi + k_1\epsilon_e/\epsilon_1 = 0 \quad (7)$$

with

$$k_1^2 = -\gamma^2 - k_0^2\epsilon_1 \quad (8)$$

$$k_2^2 = -\gamma^2 - k_0^2\epsilon_e(\omega) \quad (9)$$

and

$$\gamma = \alpha + j\beta \quad (\text{complex propagation constant})$$

$$k_0^2 = \omega^2 \mu_0 \epsilon_0 \quad (10)$$

$$\epsilon_e(\omega) = \frac{\xi^2 - \eta^2}{\xi} = \epsilon^{(0)} \frac{(\omega^2 - \omega\omega_c - \omega_p^2/\epsilon^{(0)})(\omega^2 + \omega\omega_c - \omega_p^2/\epsilon^{(0)})}{\omega^2(\omega^2 - \omega_c^2 - \omega_p^2/\epsilon^{(0)})}. \quad (11)$$

The following notation has been used:

$\alpha$  attenuation constant;

$\beta$  phase constant;

$\epsilon_0$  permittivity of vacuum;

$\mu_0$  permeability of vacuum;

$\epsilon_1$  relative dielectric constant of dielectric half space;

$\epsilon_e$  effective dielectric constant of the semiconducting medium.

(Note: A propagation factor  $e^{j\omega t - \gamma z}$  has been assumed throughout.)

The expression for the effective dielectric constant of the semiconducting half-space given above corresponds to the lossless case. Fig. 2 shows a plot of  $\epsilon_e$  as a function of frequency. We see that  $\epsilon_e < 0$  for  $0 < \omega < \omega_0^{(1)}$  and  $\omega_\infty < \omega <$

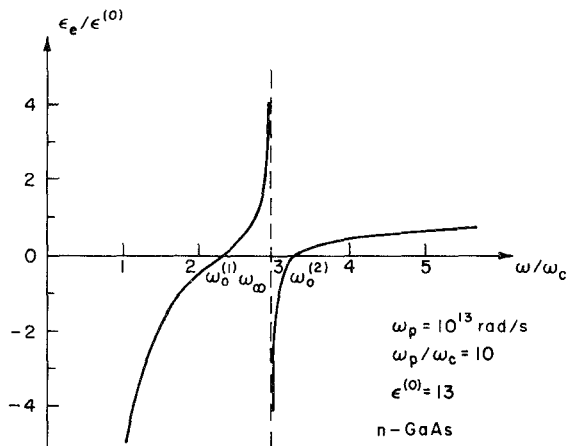


Fig. 2. Effective dielectric constant for anisotropic n-GaAs with applied uniform dc magnetic field perpendicular to the propagation direction.

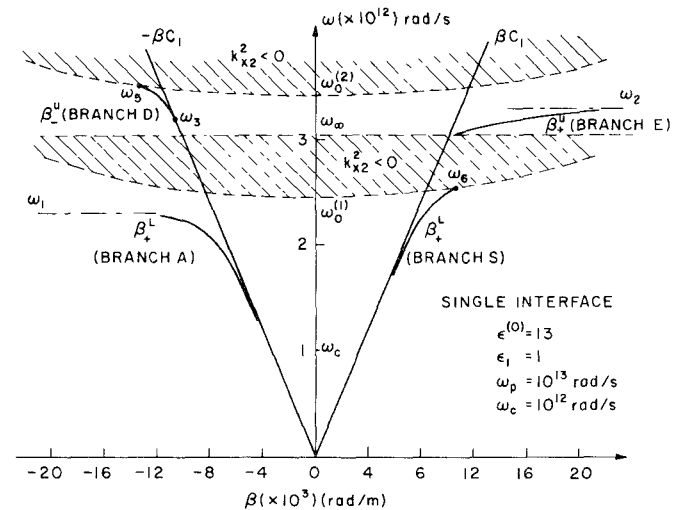


Fig. 3. Dispersion diagram of single dielectric-anisotropic n-GaAs interface. The semiconductor is assumed to be lossless

$\omega_0^{(2)}$ . Nonradiating modes are expected to occur in and near these bands. The critical frequencies  $\omega_0^{(1)}$ ,  $\omega_0^{(2)}$ , and  $\omega_\infty$  are readily obtained from (11)

$$\omega_\infty = \left( \omega_c^2 + \frac{\omega_p^2}{\epsilon^{(0)}} \right)^{1/2} \quad (12)$$

and

$$\omega_0^{(1,2)} = \frac{\pm \omega_c + \sqrt{\omega_c^2 + 4\omega_p^2/\epsilon^{(0)}}}{2}. \quad (13)$$

Fig. 3 presents a typical dispersion diagram of a dielectric-semiconductor interface wave for the lossless case ( $\nu=0$ ). The shaded areas on the diagram corresponding to  $k_2^2 < 0$  are clearly delimited. No surface wave modes can exist within them.

We see that for  $\omega_1 < \omega < \omega_6$  we have only the existence of a forward mode. This suggests the possibility of using this mode for the design of components such as isolators and even circulators, subject to the premise that, when losses and a more realistic geometry are considered, the attenua-

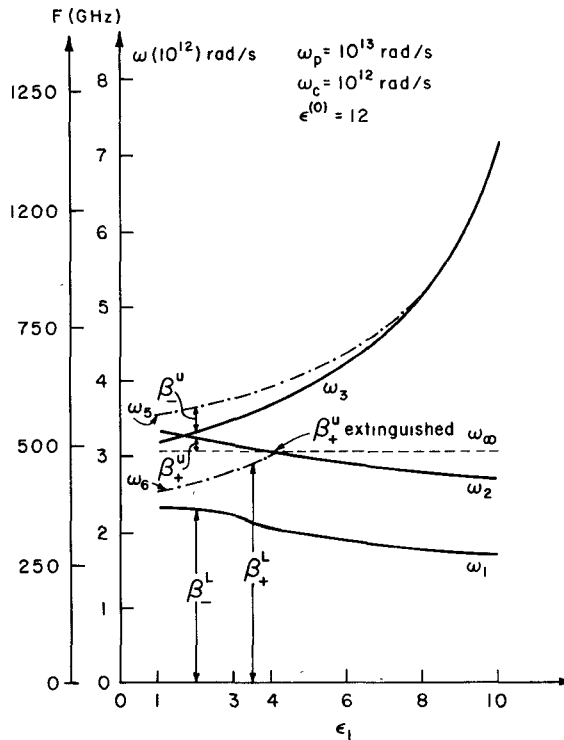


Fig. 4. Critical frequencies  $\omega_1$  to  $\omega_6$  as a function of the dielectric constant  $\epsilon_1$ , for the dielectric-anisotropic n-GaAs case (Fig. 3).

tion constant throughout this band can be made small enough.

It is to be noted that the critical frequency  $\omega_\infty$  is only a function of the semiconducting material parameters as are the curves given by  $k_2=0$ . However, the other critical frequencies,  $\omega_1$  to  $\omega_6$ , are functions of the relative permittivity of the dielectric half-space ( $x<0$ ). We can solve for all the critical frequencies explicitly in terms of  $\omega_c$ ,  $\omega_p$ ,  $\epsilon^{(0)}$  and  $\epsilon_1$  except  $\omega_5$  and  $\omega_6$  which are the roots of a quartic in  $\omega^2$ .

The bandwidths of the four branches have been examined as a function of the various parameters. A plot of the critical frequencies as functions of  $\epsilon_1$ , the relative permittivity of the dielectric half-space, is shown in Fig. 4, where the labels  $\beta_+^U$ ,  $\beta_+^L$  are used for the upper and lower branches of the forward propagation modes, respectively. Similarly, the reverse modes are labeled  $\beta_-^U$  and  $\beta_-^L$ .

We see from Fig. 4 that for isolation and circulation—with suppression of unwanted modes—modest dielectric loading is indicated. This would reduce the bandwidths of  $\beta_+^U$  and  $\beta_-^L$ , extinguish  $\beta_+^U$  and give maximum bandwidth to  $\beta_+^L$  by achieving considerable separation between  $\omega_1$  and  $\omega_6 \approx \omega_\infty$ . We may attain  $\omega_6 = 2\omega_1$ .

Also, as we increase  $\epsilon_1$  and have  $\beta_+^U$  vanish, at the same time  $\beta_+^U$  is restricted to a small region close to the light line at the lower end of the band and close to the  $k_2=0$  curve at the upper end. At the lower end of the band then the mode extends considerably into the dielectric region while at the upper end the transverse field distribution is almost constant in the semiconducting half-space.

Similarly, the lower branches will be close to the light

line for a considerable part of the band as we increase the dielectric loading, with the attendant spreading of the field into the dielectric region.

### III. THE SLAB

A geometry that offers a better model for practical applications is a thin film of semiconducting material sited by dielectric.

If the semiconducting region is thin enough, important modifications to the results studied in the last section will take place. First, when the effects of losses in the semiconductor are considered, we expect the attenuation constants of the different modes to be greatly reduced, in contrast with the semi-infinite structure, as less electromagnetic energy travels inside the thin plasma region. Second, if the slab is thin enough, there will be a strong coupling between the interface waves that propagate on both surfaces of the slab. This feature is most significant when the semiconducting medium is made anisotropic, as is here the case.

The geometry to be studied is given in Fig. 1(b), where a uniform dc magnetic field  $B_0$  is applied in the  $y$ -direction. For the fields to be confined to the vicinity of the slab their transverse behavior in regions 1 and 3 must be given by  $e^{k_1 x}$  and  $e^{-k_3 x}$ , respectively, with

$$\operatorname{Re}[k_1] > 0 \quad \operatorname{Re}[k_3] > 0. \quad (14)$$

Inside the slab the fields have the general form

$$Ae^{k_2 x} + Be^{-k_2 x}. \quad (15)$$

The dispersion relation for this guiding system is

$$e^{-2k_2 w} - \frac{(k_2 + j\gamma\eta/\xi + k_2\epsilon_e/\epsilon_1)(k_2 - j\gamma\eta/\xi + k_3\epsilon_e/\epsilon_3)}{(k_2 - j\gamma\eta/\xi - k_1\epsilon_e/\epsilon_1)(k_2 + j\gamma\eta/\xi - k_3\epsilon_e/\epsilon_3)} = 0 \quad (16)$$

where

$$k_3^2 = -\gamma^2 - k_0^2\epsilon_3 \quad (17)$$

$w$  is the slab width and the other parameters have been defined previously.

We first study the case of symmetric loading, i.e., when  $\epsilon_1 = \epsilon_3$ . Fig. 5 shows typical results for a slab placed in vacuum. Because of the geometric symmetry of the structure so also is the  $\omega$ - $\beta$  diagram symmetric about the frequency axis.

At first we will not consider the slab to be lossy. The effects of taking a finite collision frequency  $\nu$  will be considered later on in this section.

We must first take notice of the fact that  $k_2^2$  can be either greater or less than zero, which gives hyperbolic or trigonometric transverse field distributions in the slab, respectively. The regions of  $k_2^2 > 0$  and  $k_2^2 < 0$  are clearly delimited in the  $\omega$ - $\beta$  diagram of Fig. 5.

Comparing Figs. 3 and 5, those modes that in the single interface case terminated on the  $k_2=0$  curves, now no longer do so; rather, they make a smooth transition from a hyperbolic to a trigonometric field distribution. The primary effect of this is that the bandwidth of the upper

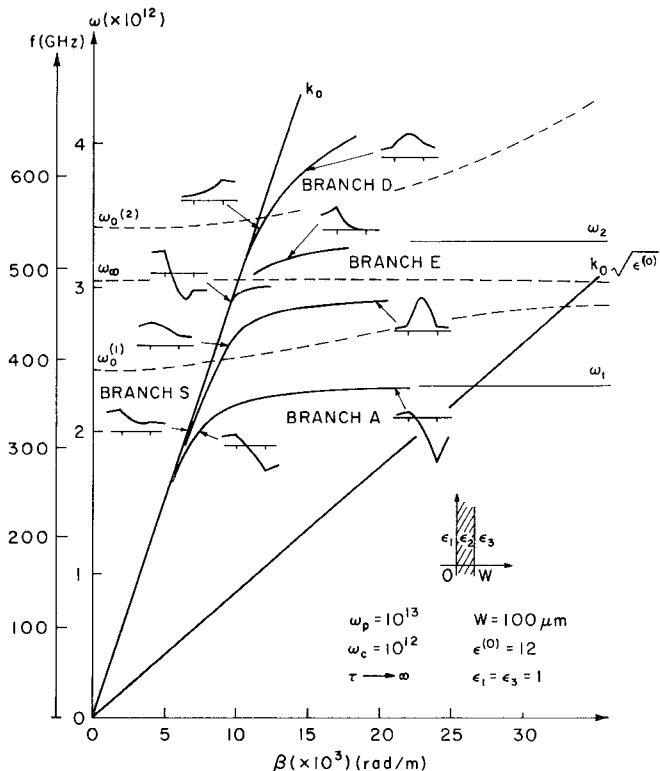


Fig. 5. Dispersion diagram for the symmetrically loaded anisotropic n-GaAs slab. The semiconductor is assumed to be lossless.

branch mode (branch *D*) is now extended without limit and ultimately becomes asymptotic to the light line for the semiconductor, i.e.,  $\omega = k_0 \sqrt{\epsilon^{(0)}}$ . The lower branch (branch *S*), which previously was quenched now becomes asymptotic to the frequency  $\omega_\infty$ .

Branches *E* and *A* remain the same. The only additional modes found are the "volume" modes in the region where  $k_2^2$  is negative and where the effective permittivity is large and positive. These modes show trigonometric behavior, have little or no field displacement and their energy is dominantly concentrated within the semiconducting slab. It is clear then that when we introduce material losses these modes will be heavily attenuated since they occur near the frequency where we will have the material resonance.

For branches *A*, *S*, *D*, and *E* we find a field displacement effect, particularly in the areas where  $k_2^2 > 0$ . This can be seen in Fig. 5 where the transverse behavior of the magnetic field component is plotted for several points of the  $\omega - \beta$  diagram. We find that for the forward propagation direction the field adheres to the face at  $x=0$  for branches *S* and *E*, while for branches *A* and *D* it clings to the face at  $x=W$ . For the opposite direction of propagation the displacement is reversed.

If the semiconducting slab is thought of as being infinitely wide, the propagation characteristics of the fields in a given direction would be that of two single interfaces supporting surface waves of opposite propagation directions. That is, the dispersion diagram obtained would be that of a single interface whose  $\beta < 0$  half-plane has been

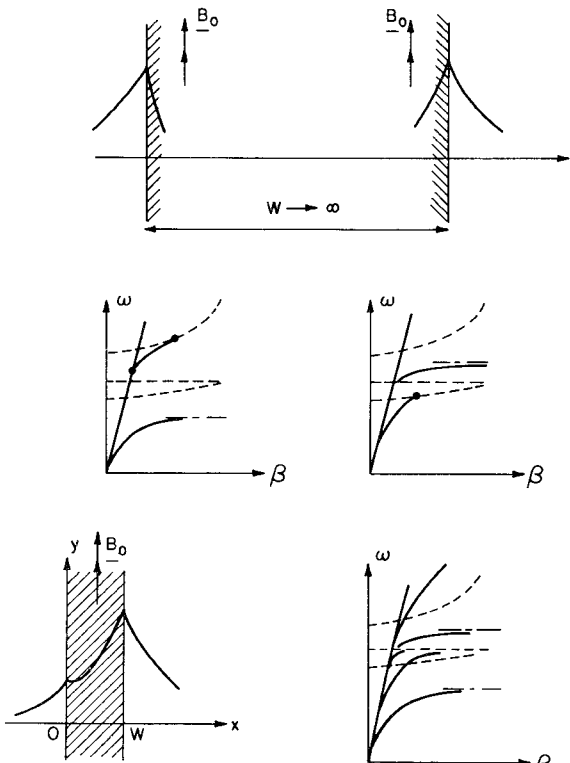


Fig. 6. The field displacement effect.

folded over to the  $\beta > 0$  side (see Figs. 3 and 6). This  $\omega - \beta$  diagram is modified to that of Fig. 5 when the width of the slab is reduced and we obtain coupling between the fields that cling to each surface. Notice that, inside the semiconductor the fields decay exponentially and that the rate of decay is now small compared to the width of the slab.

As branches *S* and *A* (Fig. 5) tend to the light line for lower values of  $\omega$  we see from the field structure that they approach symmetric and antisymmetric modes for the isotropic limit case, respectively [24]. The upper branches behave differently. Branch *E* has essentially a surface mode structure with dominant electric field strength (i.e., it is a quasi-electrostatic mode). On the other hand, branch *D* also has the structure of a surface mode at the low end of the band but gradually, as frequency increases, the fields are distributed more uniformly throughout the semiconducting medium. This mode is thus very similar to the dynamic mode found for the case of ferrites [25]–[27].

We have thus justified the labeling of the four surface modes found with the letters *S* (symmetric), *A* (antisymmetric), *E* (electrostatic), and *D* (dynamic).

We consider next the case of loading the sides of the semiconducting slab with two different dielectrics. Since the slab must be supported by some kind of substrate, the case  $\epsilon_1 > 1, \epsilon_3 = 1$  would be nearest to a practical structure which could model differential phase shifters and possibly circulators.

A sample result is presented in Fig. 7 for the configuration shown in the insert. We study here the lossy case with

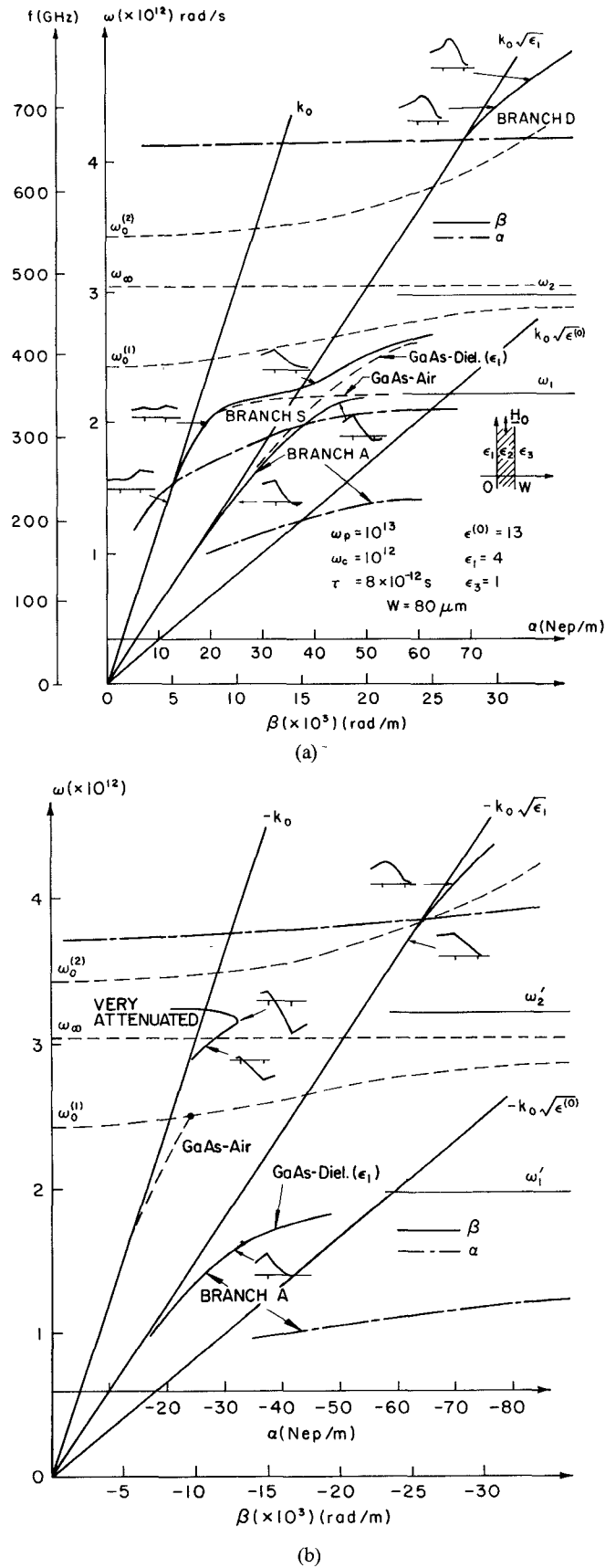


Fig. 7. (a) Dispersion diagram for the asymmetrically loaded lossy anisotropic n-GaAs slab. Forward propagation direction. (b) Dispersion diagram for the asymmetrically loaded lossy anisotropic n-GaAs slab. Reverse propagation direction.

$\tau = 1/\nu = 8 \times 10^{-12}$  s and, therefore, the propagation constant will now be complex, i.e.,  $\gamma = \alpha + j\beta$ .

The dashed lines in Fig. 7 correspond to the GaAs-dielectric ( $\epsilon_1 = 4$ ) and GaAs-vacuum ( $\epsilon_3 = 1$ ) single interface cases, respectively (see Fig. 3).

As before, the wave propagation in the GaAs slab can be viewed as the interaction between the surface waves supported by the two interfaces. Indeed, for a thicker semiconducting slab, branches *A* and *S* move closer to the single interface modes. In the forward propagation direction, the fields corresponding to modes *A* and *S*, which at sufficiently low frequencies adhere to opposite interfaces, experience, as frequency increases, a transition in which the field energy is redistributed to the opposite interface. Accordingly, we see that when the transition is completed, branches *A* and *S* approach the single interface modes corresponding to the slab face to which the fields now cling.

In the short frequency range over which this transition occurs, the attenuation constants of both modes *A* and *S* increase considerably as more energy travels inside the GaAs slab, the only source of losses.

For the reverse propagation (Fig. 7(b)) we see that only branch *A* exists. This is confirmed by the GaAs-vacuum interface dispersion curve, which exists entirely between the light lines in region 1 ( $\epsilon_1 = 4$ ) and vacuum. It must be stressed here that Maxwell's equations do not allow for bounded modes to exist in this region of the  $\omega - \beta$  plane. However, branch *S* is a bounded mode due to the effect of losses in the GaAs slab, with fields extending far into the high dielectric region, away from the slab.

The poor confinement of the fields to the vicinity of the semiconducting slab is the primary disadvantage to the use of branch *S* for practical purposes. On the other hand, it exhibits a lower attenuation constant than the other modes found (0.56 dB/mm, at 330 GHz, or less) and is unidirectional. Hence, this mode is particularly attractive for the design of isolators and directional couplers.

Branch *A*, in turn, offers possibilities for differential phase shifter design ( $\Delta\phi = 300^\circ/\text{mm}$  at 285 GHz) provided branch *S* is suppressed and ways can be found of reducing the high attenuation constant which branch *A* exhibits. This can be done either by improving the quality of the material or by modifying the configuration so as to guide more of the energy outside the GaAs slab.

Branch *D*, for both directions of propagation, exists almost entirely within the region  $\text{Re}[k_2^2] < 0$  which corresponds to a trigonometric distribution of the fields within the slab. Hence, due to the semiconductor losses, this mode is highly attenuated.

Branch *E* is also highly attenuated and is not included in Fig. 7.

A new geometry, now under consideration, is aimed at improving the performance of branches *A* and *S* for modeling phase shifters and isolators, respectively. It consists of a dielectric slab parallel to the semiconducting slab and placed at a certain distance from it. The structure param-

ters may then be varied so as to be able to control the fraction of energy which is carried external to the semiconducting slab, as well as the amount of dielectric loading on one side of the GaAs slab.

The results of a study of such a five-region canonical structure will be reported on in a future paper.

#### IV. CONCLUSION

The surface waveguiding properties of anisotropic semiconducting plasma have been studied and the performance of millimeter and near-millimeter nonreciprocal devices explored. A moderately doped polar semiconductor of high material quality ( $\omega_p = 10^{13}$  rad/s,  $\tau = 8 \times 10^{-12}$  s) such as n-GaAs is used as the solid state plasma medium.

Two basic geometries have been considered: a single semiconductor-dielectric interface and a semiconducting slab sided by dielectric. The different propagation modes existing in such structures and the corresponding field configurations and their properties were investigated. For the case of the semiconducting slab, the field displacement effect, already observed in ferrites, was found to occur for four of the propagation modes. The utility of some of these modes for design of isolators, circulators, phase shifters, and directional couplers was considered.

Special attention has been given to the anisotropic semiconducting slab sided by vacuum and dielectric. This geometry more closely models a practical structure where the guiding structure must be supported or contained by a substrate.

A more complicated five-region canonical structure is being investigated and will be reported on shortly.

#### ACKNOWLEDGMENT

We wish to thank Dr. A. V. Nurmikko for his contribution to our understanding of the fundamental properties of solid-state plasma phenomena on which this work is based. We are also indebted to Mrs. W. L. Hwang for her collaboration in generating numerical data and for useful discussions on the material covered in Section III of this article.

#### REFERENCES

- [1] N. W. Ashcroft and N. D. Mermin, *Solid State Physics*. New York: Holt, Rinehart and Winston, 1976.
- [2] C. Kittel, *Introduction to Solid State Physics*. New York: Wiley, 1976.
- [3] B. Lax, "Magneto-plasma effects in solids," *IRE Trans. Microwave Theory Tech.*, vol. MTT-9, pp. 83-89, Jan. 1961.
- [4] J. J. Brion, R. F. Wallis, A. Hartstein, and E. Burstein, "Theory of surface polaritons in anisotropic dielectric media with applications to surface magnetoplasmons in semiconductors," *Phys. Rev. B*, vol. 9, pp. 3424-3437, Apr. 1974.
- [5] E. N. Economou, "Surface plasmons in thin film," *Phys. Rev.*, vol. 182, pp. 539-551, June 1969.
- [6] J. J. Brion, R. F. Wallis, A. Hartstein, and E. Burstein, "Interaction of surface magneto-plasmons and surface optical phonons in polar semiconductors," *Surf. Sci.*, vol. 34, pp. 73-80, 1973.
- [7] —, "Theory of surface magneto-plasmons in semiconductors," *Phys. Rev. Lett.*, vol. 28, pp. 1455-1458, May 1972.
- [8] B. G. Martin, A. A. Maradudin, and R. F. Wallis, "Theory of damped surface magneto-plasmons in n-type InSb," *Surf. Sci.*, vol. 77, pp. 416-426, 1978.
- [9] J. J. Quinn and K. W. Chiu, "Magneto-plasma surface waves in

metals and semiconductors," in *Polaritons, Proc. 1st Taormina Res. Conf. Structure of Matter* (Taormina, Italy), pp. 259-268, 1972.

[10] —, "Magneto-plasma surface waves in solids," *Il Nuovo Cimento*, vol. 10B, pp. 1-20, July 1972.

[11] —, "Magneto-plasma surface waves in polar semiconductors: Retardation effects," *Phys. Rev. Lett.*, vol. 29, pp. 600-603, Aug. 1972.

[12] —, "Magneto-plasma surface waves in metals," *Phys. Rev.*, vol. 5, pp. 4707-4709, June 1972.

[13] A. Hartstein, E. Burstein, J. J. Brion, and R. F. Wallis, "Surface polaritons on semi-infinite anisotropic media," *Surf. Sci.*, vol. 34, pp. 81-89, 1973.

[14] A. S. Barber, "Response functions for surface polaritons at interfaces in solids," *Surf. Sci.*, vol. 34, pp. 62-72, 1973.

[15] J. Schoenwald and E. Burstein, "Propagations of surface polaritons at optical frequencies over macroscopic distances along semi-infinite interfaces," in *Polaritons, Proc. 1st Taormina Res. Conf. Structure of Matter* (Taormina, Italy), pp. 139-145, 1972.

[16] B. Fischer, N. Marschall, and H. J. Queisser, "Experimental studies of optical surface excitations," *Surf. Sci.*, vol. 34, pp. 50-61, 1973.

[17] P. K. Cibin, "Propagation of guided electron plasma waves on a planar plasma slab in the presence of dissipative processes," *Phys. Lett.*, vol. 70A, pp. 103-104, Feb. 1979.

[18] J. N. Maiti and J. Basu, "Properties of a dielectric-Rod waveguide immersed in plasma," *J. Appl. Phys.*, vol. 45, pp. 1650-1656, Apr. 1974.

[19] R. E. Hayes and W. G. May, "The use of semiconductors in nonreciprocal devices for submillimeter wavelengths," in *Proc. Symp. Submillimeter Waves*, Polytechnic Inst. Brooklyn, pp. 237-250, 1970.

[20] B. R. McLeod and W. G. May, "A 35 GHz isolator using a coaxial solid-state plasma in a longitudinal magnetic field," *IEEE Trans. Microwave Theory Tech.*, vol. MTT-19, pp. 510-516, June 1971.

[21] M. Kanda and W. G. May, "Nonreciprocal reflection-Beam isolators for far-infrared use," *IEEE Trans. Microwave Theory Tech.*, vol. MTT-21, pp. 786-790, Dec. 1973.

[22] —, "Hollow-cylinder waveguide isolators for use at millimeter wavelengths," *IEEE Trans. Microwave Theory Tech.*, vol. MTT-22, pp. 913-917, Nov. 1974.

[23] —, "A millimeter-wave reflection-beam isolator," *IEEE Trans. Microwave Theory Tech.*, vol. MTT-23, pp. 506-508, June 1975.

[24] A. V. Nurmikko, D. M. Bolle, and S. Talisa, "Guiding and control of millimeter waves by surface plasmon phenomena in semiconductors," *Int. J. Infrared Millimeter Waves*, vol. 1, pp. 1-11, Jan. 1980.

[25] G. Forterre, B. Chiron, and L. Courtois, "A survey of broad band stripline ferrite isolators," *IEEE Trans. Magn.*, vol. MAG-11, pp. 1279-1281, Sept. 1975.

[26] P. DeSantis, "A unified treatment of edge-guided waves," *Naval Research Laboratory*, Washington DC, NRL Rep. 8158, Washington DC, Jan. 1978.

[27] S. H. Talisa and D. M. Bolle, "On the modeling of the edge-guided mode stripline isolators," *IEEE Trans. Microwave Theory Tech.*, vol. MTT-27, pp. 584-591, June 1979.



**Donald M. Bolle** (S'56-M'57-SM'66) was born in Amsterdam, The Netherlands, on March 30, 1933. He received the B.Sc. degree with honors in electrical engineering from Kings College, Durham University, England, in 1954, and the Ph.D. degree in electrical engineering from Purdue University, West Lafayette, IN, in 1961.

From 1954 to 1955, he was a Research Engineer with the Electrical Musical Industries, Middlesex, England. He taught at Purdue University from 1956 to 1962, first as an Instructor, then as an Assistant Professor in Electrical Engineering. He spent the academic year 1962-1963 in the Department of Applied Mathematics and Theoretical Physics, Cambridge University, England, as an NSF Postdoctoral Fellow. In 1963, he joined Brown University, Providence, RI, where he was Professor of Engineering. Presently, he is the Chandler Weaver Professor and Chairman of the Department of Electrical and Computer Engineering at Lehigh University, Bethlehem, PA. He will hold

the position of Dean of the College of Engineering and Physical Sciences at Lehigh University effective July 1, 1981. Currently he is President of the IEEE Council on Oceanic Engineering. He was a Visiting Professor at the Institute for High-Frequency Techniques of the Technical University of Braunschweig, Germany, in 1967, at the University of Colorado, Boulder, in 1972 and Senior Research Fellow and Visiting Professor at University College, University of London, London, England, for the fall semester of the academic year 1979-1980. His present research interests lie primarily in the near-millimeter components.

Dr. Bolle is a member of Eta Kappa Nu, Tau Beta Pi, Sigma Xi, ASEE, AAAS, and AAUP. He is currently Editor in Chief of the IEEE TRANSACTIONS ON OCEANIC ENGINEERING.



and propagation.

**Salvador H. Talisa** (M'76) was born in Lima, Perú, on December 17, 1951. He received the degree of electrical engineering from the Escuela Técnica Superior de Ingenieros de Telecomunicación de Barcelona, Spain, in 1976, the Sc.M. degree from Brown University, Providence, RI, in June 1978, and is presently working towards the doctoral degree.

He joined the Division of Engineering, Brown University, in 1976, as a Research Assistant. His interests lie in the area of electromagnetic theory

# A Hybrid Method for Paraxial Beam Propagation in Multimode Optical Waveguides

DAVID C. CHANG, SENIOR MEMBER, IEEE, AND EDWARD F. KUESTER, MEMBER, IEEE

**Abstract**—A hybrid (nonray, nonmodal) method for computing the fields of a paraxial beam propagating in a multimode waveguide (parallel-plate or dielectric slab) at large axial distances is presented. The method is based on the Fourier and Fresnel self-imaging properties of these waveguides, and is capable of high accuracy. The method is much more efficient than ray or mode approaches, while giving complete field information which coupled-power equations do not provide.

## I. INTRODUCTION

**M**ULTIMODE optical fibers appear at present to be the most common optical waveguiding medium for applications in the immediate future. Incoherent sources and relatively simple detectors can be used, and the tolerance problems encountered with single-mode fibers are far less severe with such waveguides.

At present, there are essentially three methods available for field computation in multimode waveguides. First, one can take a pure modal approach—the excitation amplitude of each mode is computed, and all modes are summed together. Although in principle exact, this approach suffers not only from the large number of modes which must be

kept track of (100~1000 for a typical fiber; 30~100 for a slab geometry) but also from a large degree of cancellation of terms in the mode sum when the field does not match that of an individual mode. Examples of the application of this method may be found in [1]. Although in some special cases approximate closed-form results are available, a computer analysis is generally required, and roundoff errors can be expected to accumulate, especially for large propagation distances.

A second approach is that of geometrical optics (sometimes encountered as the WKB method). An excellent discussion of this approach has been given by Gloge and Marcatili [2] (see also [3]). Here one approximates the effect of a large number of discrete propagating modes by a continuously distributed propagation constant belonging to a “continuous spectrum” of modes. These, when computed under the WKB approximation, can be interpreted as a cone of rays lying within some characteristic acceptance angle of the fiber. The propagation problem then reduces to that of determining the amplitude with which each ray is excited, and tracing it down the length of the guide. Intuitively more suitable for multimode guides because of the “high-frequency” nature of the problem, this approach is nonetheless approximate by virtue of the geometrical optics technique. Moreover, in a situation where

Manuscript received December 12, 1980; revised April 10, 1981. This work was supported by Army Research Office (ARO) under Grant DAAG 29-G-0173, monitored by Dr. J. Mink.

The authors are with the Electromagnetics Laboratory, Department of Electrical Engineering, University of Colorado, Boulder, CO 80309.